Supplementary Information (SI) for Journal of Materials Chemistry C.
This journal is © The Royal Society of Chemistry 2025
Please do not adjust margins

ARTICLE

Supplemental Material

Received 00th January 20xx,
Accepted 00th January 20xx

DOI: 10.1039/x0xx00000x

Frequency-Reconfigurable Conformal Metastructure with Liquid Crystal Temperature Control for RCS Reduction

Shuo Dai, Si-Yuan Liao, Jun-Rui Pan, and Hai-Feng Zhang

1. Temperature Control of Liquid Crystal

1.1 Liquid Crystal heating method

A thermocouple is a widely used temperature sensor known for its ability to detect temperature changes with high sensitivity [1]. The heater power incorporates a ceramic heater, with the sample mounted on its upper surface and a thermocouple embedded within. The entire assembly is enclosed in a vacuum chamber. Utilizing the oil bath heating method, the thermocouple's cold end can maintain a stable temperature of 0.5°C, enabling a precise single-valued temperature function for accurate measurement. Additionally, the internal structure features a black surface, effectively minimizing infrared reflection and enhancing thermal efficiency. By adjusting the input power to the heater, the heat load on the sample can be modified. Combined with the thermocouple's temperature measurements, this setup allows for precise control of the heating temperature. The specific structure diagram is shown in Fig.S1.

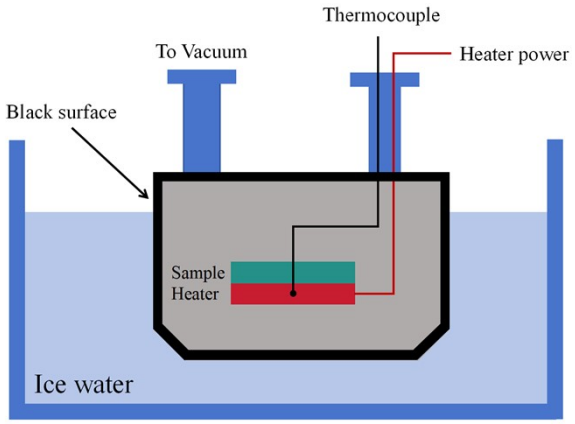

Fig.S1 Schematic diagram of vanadium dioxide heating device

1.2 Liquid Crystal heating method

The liquid crystal employed in S-shaped absorber (SA) is a temperature-controlled type, and precise thermal regulation is achieved through a thermocouple heating method based on an oil bath system (see in FIg.S1(a)). The absorption spectrum at 40 °C is presented in Fig.S2(a), where a noticeable difference is observed between the absorption of TE and TM waves. For TE waves, broadband absorption is achieved across the 1.39–18 GHz range, while for TM waves, broadband absorption generally spans from 1.65 to 18 GHz. However, in the frequency range of 13.25–13.56 GHz, the absorption falls significantly below 0.9, indicating that SA exhibits pronounced anisotropic behavior at this temperature. In contrast, at 120 °C, the absorption characteristics for TE and TM waves converge, as shown in Fig.S2(b). The comparable absorption performance of SA for both TE and TM waves at 120 °C reflects its isotropic behavior at this temperature. This behavior is primarily attributed to the variation in the dielectric constant of the liquid crystal with temperature, which alters the electromagnetic properties of SA and demonstrates its inherent reconfigurability.

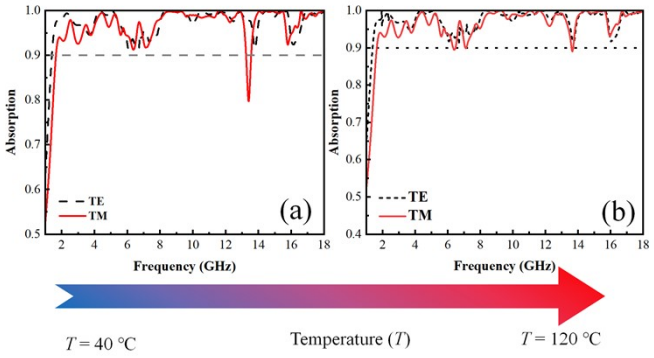

Fig.S2 Absorption spectra of SA for TE and TM waves at different temperatures. (a) 40 °C, (b) 120 °C

[a] *Hai-Feng Zhang is the corresponding author, who is with College of Electronic and Optical Engineering and the College of Flexible Electronics (Future Technology), Nanjing University of Posts and Telecommunications, Nanjing, 210023, China. (*e-mail: hanlor@njupt.edu.cn or hanlor@163.com).*
[b] *The other authors are with College of Electronic and Optical Engineering and the College of Flexible Electronics (Future Technology), Nanjing University of Posts and Telecommunications, Nanjing, 210023, China.*

Please do not adjust margins

Please do not adjust margins

2. The fabrication process of SA

In this section, the feasibility of the SA fabrication scheme is evaluated. Due to the limitation of experimental resources and equipment, we are unfortunately unable to fabricate this superstructure independently. Therefore, we will provide relevant references for each step to support the fabrication process of the metastructure.

The millimeter-scale dimensions of the SA ensure its high feasibility for practical fabrication. The total diameter of the absorber is 373 mm, with a spherical shell thickness of 5.5 mm, and even the smallest structural gap exceeds 1 mm—tolerances that are well within the capabilities of current industrial manufacturing technologies. The primary fabrication challenges lie in constructing the S-shaped geometry and vertically printing the spiral pattern onto the substrate. To address these issues, we referred to relevant prior studies that demonstrate feasible solutions for such fabrication processes. As illustrated in Fig.S3, the proposed manufacturing process involves three main steps:

Step (a): A rectangular substrate composed of AP is prepared and subsequently fabricated into an S-shaped structure using 3D printing technology [2]. Numerous approaches exist for manufacturing S-shaped structures, particularly at the millimeter scale. Among these, 3D printing is the most widely adopted method due to its precision and flexibility [2]. Additionally, existing studies have demonstrated that ceramic substrates can be shaped into complex geometries using 3D printing with accuracies reaching 0.02 mm [3]. Compared to such intricate structures, for example, gyroscopic geometries [3], the S-shaped structure employed in this work is significantly larger and simpler, thereby offering greater ease of fabrication and structural advantages.

Step (b): A copper film is deposited on the back surface of the S-shaped structure using a wet chemical coating process, as demonstrated in previous studies [4]. Ishikawa *et al*. [4] successfully applied a 0.04 mm-thick silver film onto a three-dimensional substrate using this method. The same coating technique is applicable to the SA design presented in this paper, providing a reliable approach for metal layer deposition on complex geometries.

Micron-sized particles with a diameter of 8 μm are uniformly mixed with an adhesive to form a sealing ring with a height of 0.1 mm on the upper surface of the first AP layer [5]. A small hole is intentionally left on one side of the ring to enable the injection of the liquid crystal material.

Step (c): The upper S-shaped AP layer with a thickness of 0.3 mm is fabricated using 3D printing technology [2]. This upper AP layer is then pressed onto the adhesive layer to form a liquid crystal cavity. The liquid crystal material is subsequently injected into the cavity through the pre-designed hole [5].

Step (d): A layer of conductive ink with a sheet resistance of 280 Ω/sq is printed on the inner surface of the S-shaped structure using pad printing technology [6]. Considering the need for vertical printing on the inner side of the S-shaped structure, an effective solution is pad printing technology, which allows printing special patterns on irregular surfaces [6]. Wu *et al*. reported a pad printing technology [7] in which the conductive material was picked up from a flat spiral pattern mold through a silicone pad and then transferred to a hemispherical PMMA substrate (24 mm outer diameter, 1 mm thickness). The thickness of the printed arm was about 0.02 mm. This level of accuracy is very suitable for SA. These spiral pattern molds can be manufactured using 3D technology to etch grooves on a plastic flat plate [7].

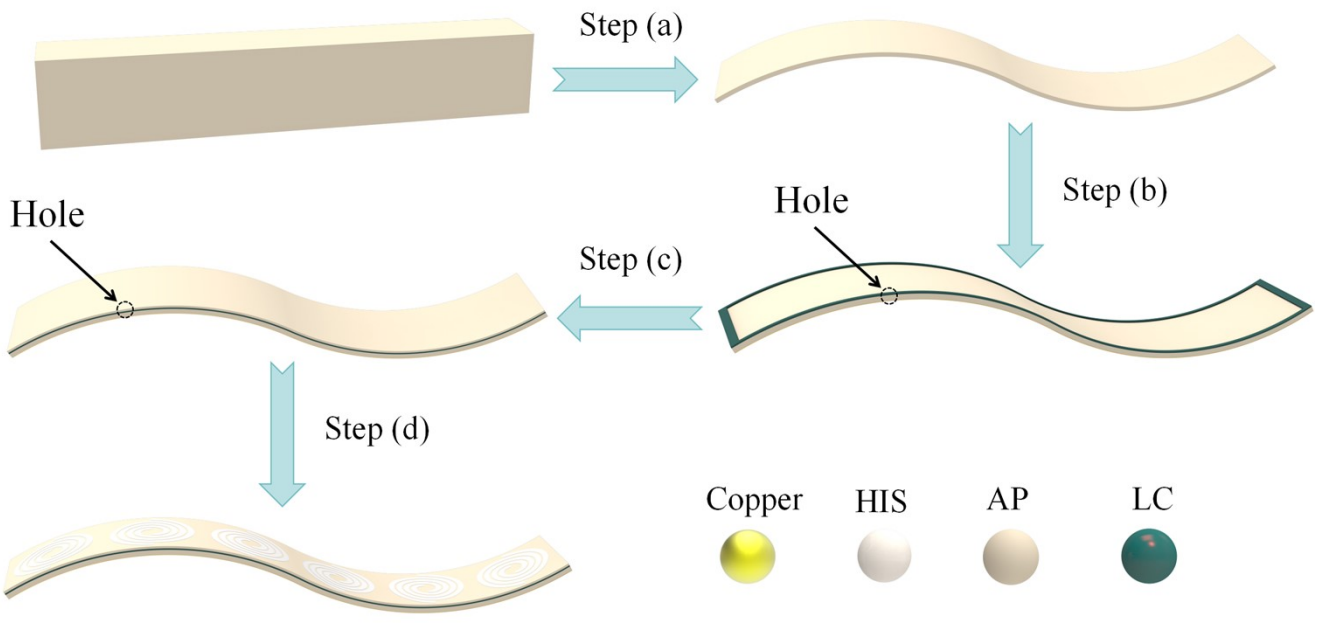

Fig.S3 Detailed fabrication process of SA.

Notes and references

1. E. Leonidas, S. Ayvar-Soberanis, H. Laalej, S. Fitzpatrick and J. R. Willmott, Sensors, 2022, **22**, 4693.
2. J.H. Park, J.R. Lee, Polymers. 2019, **11**, 1800.
3. L. Yao, W. Yang, S. Zhou, H. Mei, L. Cheng, L. Zhang, Carbon, **196**, 961-71.
4. A. Ishikawa, T. Kato, N. Takeyasu, K. Fujimori, K. Tsuruta, Applied physics letters, **111**.
5. Q.J. Li, S.Y. Liao, F.Z. Liu, H.F. Zhang, Physics of Fluids, **36**.

This journal is © The Royal Society of Chemistry 20xx

Please do not adjust margins

Please do not adjust margins

6. M. Sato, M. Ohnishi, T. Abe, InNIP & Digital Fabrication Conference, **27**, 478-481.
7. H. Wu, S.W. Chiang, C. Yang, Z. Lin, J. Liu, K.S. Moon, F. Kang, B. Li, C.P. Wong, PloS one, **10**, e0136939.
8. A. Álvarez-Trejo, E. Cuan-Urquizo, D. Bhate, A. Roman-Flores, Materials & Design, **233**, 112190.

This journal is © The Royal Society of Chemistry 20xx

Please do not adjust margins